International Journal of Engineering, Mathematical and Physical Sciences
ISSN: 2517-9934
Vol:7, No:1, 2013

Wave Vortex Parameters as an Indicator of Breaking Intensity

B. Robertson, and K. Hall

***Abstract*—**The study of the geometric shape of the plunging wave enclosed vortices as a possible indicator for the breaking intensity of ocean waves has been ongoing for almost 50 years with limited success. This paper investigates the validity of using the vortex ratio and vortex angle as methods of predicting breaking intensity. Previously published works on vortex parameters, based on regular wave flume results or solitary wave theory, present contradictory results and conclusions. Through the first complete analysis of field collected irregular wave breaking vortex parameters it is illustrated that the vortex ratio and vortex angle cannot be accurately predicted using standard breaking wave characteristics and hence are not suggested as a possible indicator for breaking intensity.

***Keywords*—**Breaking Wave Measurement, Wave Vortex Parameters, Analytical Techniques, Ocean Remote Sensing.

I. Introduction

OCEAN waves have fascinated and entertained us for hundreds of years. They provide us with the simplest pleasure of playing in their nearshore forms, but also are responsible for some of the greatest natural disasters on the planet. Their generation, global propagation patterns and final dissipation through breaking have intrigued and challenged scientists for over 150 years. Of all wave transformations, the moment when a wave reaches instability and begins to break is both the most complex and difficult to predict. Not all waves break in the same manner, some plunge spectacularly shooting whitewater high into the air, while others crumble slowly and quietly.

Numerous methods and theories have been used to investigate and predict the visual geometric differences between breaking wave profiles. In 1949, Iribarren and Nogales [1] proposed the Surf Similarity Parameter (SSP) to describe differences between breaking waves of similar breaker height (H_b) to depth (h_b) ratios. Based on idealized conditions, shallow water regular wave breaking events were characterized as spilling, plunging or surging waves based on wave conditions and physical inputs through Eq. (1):

$$\xi_o = \tan\alpha / \sqrt{H_o/L_o} \quad (1)$$

where α is the seafloor angle, H_o is the offshore wave height and L_o is the offshore wavelength. ξ_o values > 3.3 indicates surging waves, $0.5 < \xi_o < 3.3$ are classified as plunging breakers and $\xi_o > 0.5$ define spilling breakers. The SSP is the benchmark for all breaking wave studies yet, in situations with non-idealized conditions, the SSP evaluation has been proven unable to differentiate between breaker types [2-6].

In an effort to quantify the physical differences within the plunging breaker category, Longuet-Higgins [7] visually analyzed the laboratory-based regular wave breaking wave profiles from Miller [8] and proposed fitting a cubic function to the enclosed vortex. Based on theoretical incompressible irrotational flow patterns, he calculated the theoretical fitted vortex length (l_v) to vortex width (w_v) aspect ratio to be 2.75 and suggested the vortex aspect ratio and angle of the fitted cubic function may be good predictor of breaking wave intensity. See Fig. 1. This suggestion was additionally corroborated by New [9].

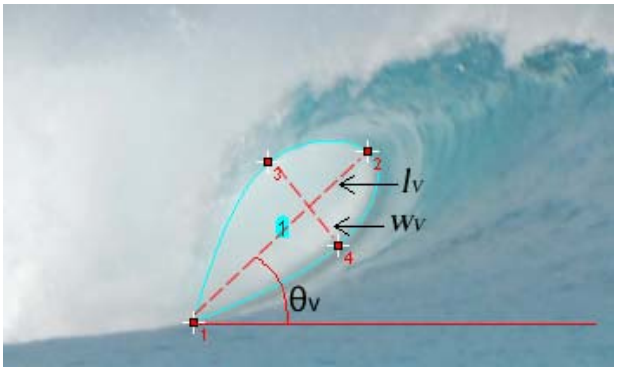

Fig. 1 Vortex Ratio and Angle

All subsequent studies investigating breaking wave vortex parameter have either recorded no direct wave data, been based on idealized theoretical solitary waves, or been conducted in laboratory wave flumes using regular waves. While laboratory wave flumes allow for direct control over wave conditions, they are also inherently limited by the scaling, surface tension and frictional effects [10]. Until this point, no studies have completed a full investigation of vortex parameters using field collected irregular breaking wave conditions over naturally varying seafloor slopes. Traditional methods of extracting of breaking characteristics from irregular waves in the field are cost prohibitive and feature poor spatial resolution. However, recent advances in remote video analysis has allowed for the collection of breaking wave positions and heights in field conditions at low costs and with high resolution [11-13].

In this paper, the feasibility of predicting breaking wave vortex parameters for use as a descriptor of breaking wave intensity is thoroughly investigated. Through the use of remote and in-situ measurements, as well as a full bathymetric survey of the breaking zone, a complete set of breaking wave characteristic is measured in an effort to investigate and

B. Robertson is with the University of Guelph, 50 Stone Rd East, Guelph, Canada, N1G 2W1, phone: 250-891-8117 (email: bryson@uoguelph.ca)
K. Hall is with the University of Guelph, 50 Stone Rd East, Guelph, Canada, N1G 2W1, phone: 519-824-4120 ext 53081 (email: k.hall@exec.uoguelph.ca).

quantify any possible trends between breaker vortex parameters and incoming wave conditions.

II. Published Vortex Parameter Predictors

In the first detailed study based on the suggestions of Longuet-Higgins and New, Mead and Black [2] fitted a cubic function to 46 pre-published images of wave vortex profiles at 23 plane emergent beaches and barred reefs worldwide. Resulting vortex ratios varied between 1.73 and 3.43 and vortex angles between 29° and 58°. Given that no direct wave data were collected, they proposed that the vortex ratio is independent of wave characteristics and depends only on the orthogonal slope, according to:

$$Y = 0.065m' + 0.821 \quad (2)$$

where $m' = m\cos\varphi$, m' is the seafloor slope normal gradient and φ is the peel angle of the wave measured with respect to the wave ray [14]. The seafloor slopes 2 - 3m shallower and 2 - 3m deeper than an estimated break point were averaged to estimate the effective seafloor slope. Table I details the breaking intensity categories.

TABLE I
Breaking Intensity Categories

Intensity	Extreme	Very High	High	Medium High	Medium
Vortex Ratio (Y)	1.6 – 1.9	1.9 – 2.2	2.2 – 2.5	2.5 – 2.8	2.8 – 3.1

Mead and Black found a coefficient of correlation (R^2) value of 0.71 using their collected data and Eq. (2), illustrating the possibility that the vortex ratio may be a defining breaking wave intensity characteristic. Mead and Black were unable to find dependence between the vortex angle and any combination of slope and vortex parameters. No direct wave measurements were collected.

In 1997, Grilli, Svendsen and Subramanya [6] presented breaking wave profiles from a fully non-linear potential flow wave model (FNPM), which input three offshore solitary wave steepness (H_o/L_o) values over four different seafloor slopes. Numerical analysis of the published figures conflicts with Mead and Black's Eq. (2), with average vortex ratios of 2.7, 2.9 and 2.1 for the 1/100, 1/35 and 1/15 slopes respectively. No vortex ratio or angle dependence on any wave characteristic could be found.

In 2007, Blenkinsopp and Chaplin [5] preformed 41 different wave flume tests over a constant 1/10 seafloor slope. The resulting vortex ratios varied between 1.46 and 2.28, despite the constant slope. Blenkinsopp and Chaplin were unable to find any vortex ratio dependencies. They note that waves with lower offshore steepness values resulted in higher vortex cavity areas yet were unable to quantify this trend due to significant data scatter.

In 2008, Fairley and Davidson [15] investigated a single steepness monochromatic wave train breaking over constant seafloor slope with varying bathymetric step sizes. In contradiction to Eq. (2), the average vortex ratios varied between 1.6 and 2.6. Their data showed vortex ratio and vortex area increased with step size. They theorized these effects are caused by lower localized seafloor slopes yet note that return flow over the steps created irregularities within their results. A poor correlation of decreasing vortex angle with increasing step size was noted.

Johnson [16] conducted detailed laboratory analysis investigating the application of the vortex ratio and vortex angles as predictors for breaking intensity. His experiments covered 4 different slopes and 72 different regular wave height and period variations. Johnson found no dependence between the vortex ratio or vortex angle and the seafloor slope, in contradiction to Eq. (2). Additionally, neither wave period nor breaking depth found correlation with the vortex ratio or angle. Only wave height was found to play a role, with smaller waves creating lower vortex ratios.

III. Field, Irregular Breaking Wave Parameter Study

In order to fully investigate the applicability of vortex parameters as indicators of breaking intensity in field conditions, a complete suite of breaking wave parameters, including breaking wave height, breaking water depth, wave period, seafloor slope, vortex angle and vortex ratio, were collected. During the fall of 2011, detailed breaking wave field studies were completed at The Hook and Sewers Peak in Santa Cruz, California and at Tropicana beach, Barbados. The aim was to collect the most accurate and detailed set of field-based, irregular wave breaking data ever assembled.

For each study location, a video camera was installed over viewing the surf zone, and recorded all wave breaking events during the study periods. The captured video footage was used to extract the position and height of individual waves at the instant their front profiles became vertical. These images were georectified, using the Matlab imtransform function and four collected ground control points, in order to transfer assign each camera pixel with real world latitude and longitude position. Hence, any manually chosen pixel from the overview video camera image could be transformed into real world co-ordinates. An example image georectification is shown in Step #1 of Fig. 2.

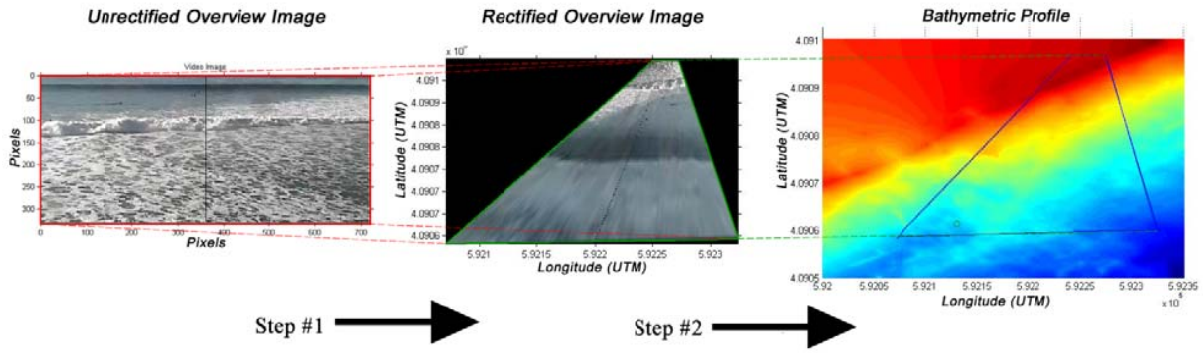

Fig. 2 Example Georectification and Bathymetric Mapping for The Hook.

In order to assess the position accuracy of the rectification process, known locations were compared against those calculated from the rectified image. For The Hook location, the average offset variation was +/- 0.85m, Sewers Peak had an average location variation of +/- 1.05m while Tropicana featured +/- 2.5m. Given that the reported accuracy of the GPS was +/- 3m, errors of this magnitude are expected and not significant.

Post georectification, every pixel based, real world latitude and longitude location was assigned a corresponding water depth (Step #2 in Fig. 2). The corresponding depths were extracted from previously collected bathymetric surveys for the study areas. For the Santa Cruz studies, bathymetric data was collect by the Unites States Geological Survey (USGS) as part of the California Seafloor Mapping Program [18], and kindly provided for this study. In Barbados, a full bathymetric survey using a 38/200 kHz Kongsberg single beam echosounder was completed. For all sites, a 500m X 500m bathymetric surface was created on a 1m x 1m grid and used to extract breaker depths and effective seafloor slopes.

Through use of the georectified image it is possible to extract the breaking wave heights and associated water depths. The automatic extraction of breaking wave heights through georectified images has been on-going since 2011 [11-13, 17], yet all published automatic algorithms suffer from substantial numbers of false positive readings due to localized atmospheric conditions and physical obstructions. In order to eliminate false positive readings, manual methods were employed in this study to choose the wave trough and wave crest pixels locations from the oblique overview video image. The corresponding real world crest (x_c) and trough (x_t) locations were calculated using the georectification matrix. Knowing x_c and x_t , the breaking wave height was calculated using the overview camera tilt angle, θ_c, and Eq. (3). Fig. 3 illustrates the basic geometry required for this calculation.

$$H_b = (x_c - x_t)\tan(90 - \theta_c) \quad (3)$$

The accuracy of this height extraction method was assessed by comparing items of known height against their calculated values. The average rectification-based uncertainties were 2.3% at The Hook, 3.9% at Sewers Peak and 2.7 % at Tropicana.

When extracting breaking wave water depths it is important to note that laboratory experiments [19] and higher order non-linear numerical wave models [20] show the wave trough position below the still water line (SWL). As result, depths extracted at the wave trough position (h_t) provided an artificially shallow water depth. Shand et al [11] suggests using $h_b=h_t+1/3H_b$ in order to correct the breaker depth to the SWL datum. This is supported by Lin et al [21] who completed a numerical study of shallow water breaking waves using Cnoidal wave theory. Numerical analysis of their published breaking figures finds the SWL breaking depth at $h_t + 0.32H_b$. As a result, all wave trough depths in this study are corrected according to the recommendations of Shand et al [11].

The manual selection of the wave trough and crest pixel locations for the breaker height and water depth calculations results in subjective errors. The human pixel choice uncertainty was assessed by manually picking pixel positions on three different occasions for every wave and found to be with +/- 1 pixel of initial choices.

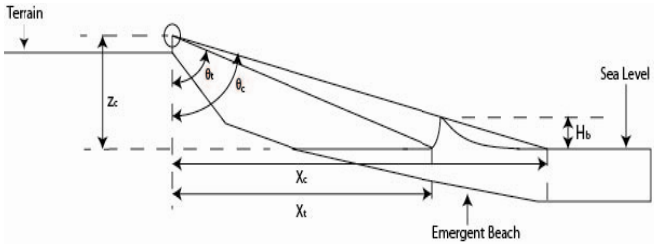

Fig. 3 Wave Height Extraction Geometry

The total height and depth uncertainties, including standard deviations (SD), were calculated by adding the independent bathymetric surface, rectification and manual method uncertainties in quadrature, according to Eq. (4). The final uncertainties are presented in Table II.

$$\sigma_{total} = \sqrt{\sigma_1^2 + \sigma_2^2 + \sigma_3^2 + \cdots} \quad (4)$$

TABLE II
TOTAL UNCERTAINTY VALUES FOR WAVE HEIGHTS AND BREAKING DEPTHS

	The Hook	Sewers Peak	Tropicana
Wave Height Uncertainty (σ_h)	4.52% (SD 0.93 %)	6.71% (SD 1.03%)	2.87% (SD 0.07%)
Water Depth Uncertainty(σ_d)	4.86% (SD 1.43%)	7.26% (SD 5.72%)	10.37% (SD 5.11%)

Wave periods were extracted from the irregular wave train via the use of a video timestack. A timestack image is constructed by extracting a single column of pixels for each video frame, and then pasting them together frame by frame, thus creating a single image for each clip of video. Fig. 4 provides an example of a timestack from Tropicana. The wave period is calculated by measuring the number of pixels between each individual wave crossing a known location, represented by the red line, and multiplying the number of pixels by the video camera frames per second (fps) rate.

Seafloor slope or gradient (1/slope) was identified as a determining factor in the breaking position, depth and shape of waves by Couriel, Horton and Cox [22]. This study followed the Coastal Engineering Manual [23] recommendations that slope should be calculated over the depth range from the point of breaking to a distance one wavelength offshore. The slopes were averaged along a curved wave ray, based on Snel's refraction law and the shallow water dispersion relation.

The performance of the collected data points, against laboratory studies, was assessed by input into the often cited and published breaker height predictors of Goda [24], Rattanapitikon and Shibayama [25] and Weggel [26]. When comparing measured and calculated breaking wave heights, the coefficients of determination (R^2) for each equation were 0.82, 0.84 and 0.84 respectively.

This indicates excellent correlation with laboratory results and confidence in the presented methods. Confident in the extraction methods and calculated values for wave height, water depth, breaking period and seafloor slope, the effect of these characteristics on the wave vortex profile were analyzed.

Raw wave vortex profiles images were captured by in-water videographers and land-based still photographers. These images were then correlated to individual waves in the video timestack via time synchronized digital image metadata. The three numbers in Fig. 4 correspond to individual wave vortex profile images. Vortex parameters were extracted on a wave-by-wave basis from photographic still images or video frame grabs of wave profiles. Using ImageJ [27], a cubic function was fitted using four defining vortex points: the point of intersection of the wave jet and wave trough (point #1), the vortex "turn-over" point (point #2), and the two points of maximum vortex width (point #3 & #4) - See Fig. 1. The final best fit vortex ratios were calculated using the length and width of the fitted cubic.

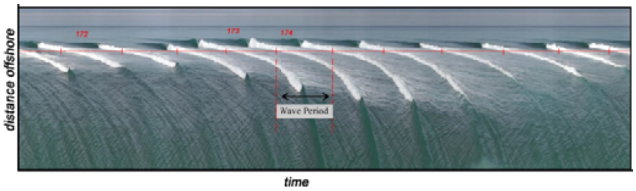

Fig. 4 Excerpt of the Tropicana video timestack.

In order to determine the reliability of the extraction process, two vortex profiles images were measured 10 times each and the resulting vortex ratios and angles were analyzed. As shown in TABLE III, the low relative uncertainties confirm this method of data extraction is sufficiently rigorous to analyze vortex ratio and angle trends. The vortex ratio measurements were consistent within ~5 % while the vortex angles were consistent within ~ 4%. The percentage uncertainty was calculated by dividing the standard deviation by the mean value.

TABLE III
VORTEX RATIO AND ANGLE EXTRACTION METHOD PRECISION

	Vortex Ratio		Vortex Angle (°)	
	Wave 1	Wave 2	Wave 1	Wave 2
Mean	2.22	2.16	45.18	42.36
Std. Dev.	0.12	0.11	1.78	1.30
Uncertainty	5.25 %	5.11 %	3.94 %	3.06 %

IV. RESULTS AND DISCUSSION

Over the 4 month data collection period, only 11 days featured significant swell activity without influencing factors such as wind, multiple swell regimes or wave reflection for vortex parameter collection. In total, 28 hours of video footage were analysed and 187 wave vortex profiles collected.

TABLE IV
VORTEX RATIO DEPENDENCE OVERVIEW

Wave Vortex Ratio Relationships				
	Constant	Slope	R-Square	Linear RMSE
Seafloor Gradient	2.03	0.01	0.27	0.25
ND Depth	2.68	-212.51	0.22	0.26
ND Wave Height	2.77	-284.2	0.18	0.26
Period	1.9	0.04	0.18	0.26
Breaker Steepness	2.83	-11.6	0.06	0.28
SSP	2.79	-0.97	0.14	0.27
Breaker Index	1.98	0.39	0.06	0.28
ND Height*Slope	2.67	-5699.77	0.26	0.25
ND Depth*Slope	2.62	-4356.65	0.28	0.25

Unfortunately, only 118 wave profiles were deemed of sufficient quality for detailed analysis. Matlab's robust fitting algorithm [28] and statistics toolbox were used to extract the linear regression fitted y –intercept, linear slope, R^2 and root-mean-square errors (RMSE) presented in Table IV. Robust fitting weights individual points based on their distance from the fitted line and eliminates the need for outlier removal. The

vertical bars in the presented plots indicate the maximum possible (Y_{max}) and minimum possible (Y_{min}) vortex ratios as an indication of possible individual vortex ratio variations.

Firstly it was noted that every incident wave at each location did not create a plunging profile despite a relatively constant effective seafloor gradient, in contradiction to Eq. (2). As shown in Fig. 5, lower seafloor gradient vortex ratios find agreement with Mead and Blacks' relationship, but increasing variation occurs as the gradient increases. The dashed regression line illustrates increasing vortex ratios with increased gradient (R^2 = 0.27) for all data points, yet when individual sites are plotted the opposite trend is evident. See Fig. 6 for an example at Tropicana. The associated vortex ratio uncertainty bars indicate large levels of uncertainty in possible trends for both plots.

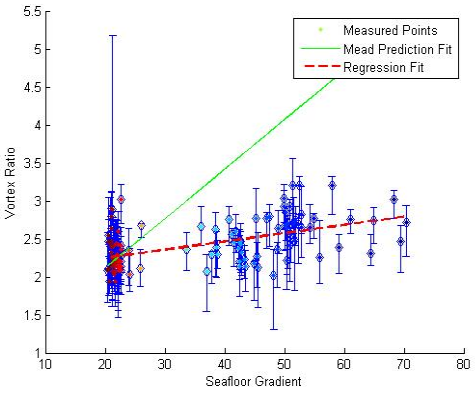

Fig. 5 Vortex Ratio vs. Seafloor Gradient

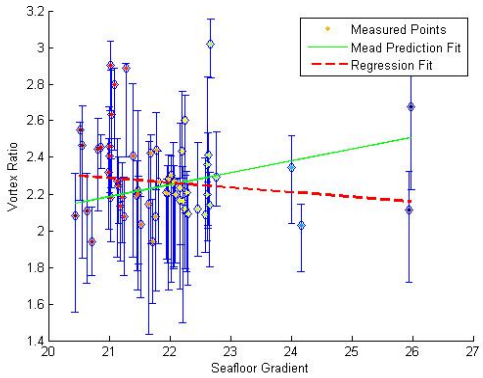

Fig. 6 Tropicana Vortex Ratio vs. Seafloor Gradient

Fig. 7 and Fig. 8 illustrate a weak decreasing vortex ratio trend with increasing non-dimensionalised wave height and breaking water depth and associated R^2 values of only 0.22 and 0.18 respectively. These trends contradict the findings of Johnson [16], who found smaller waves creating lower vortex ratios. Visual analysis of maximum and minimum possible vortex ratios illustrates large variation bounds and a subsequent lack of confidence in regression trends.

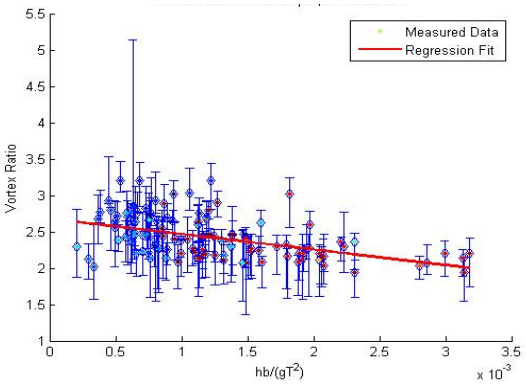

Fig. 7 ND Depth vs. Vortex Ratio Relationship

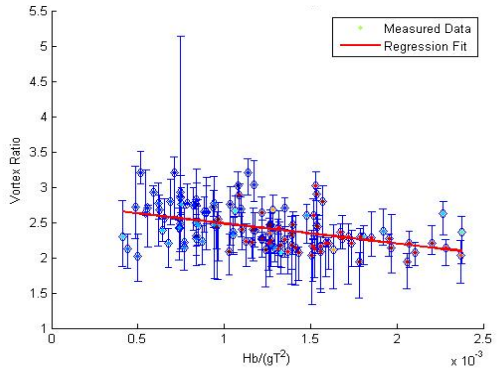

Fig. 8 ND Height vs. Vortex Ratio Relationship

Despite the regression line in Fig. 9 indicating that increasing wave periods result in small increasing vortex ratios, the R^2 value of only 0.18 indicates substantial uncertainty in this trend. The associated vortex ratio uncertainty bars indicate no significant dependence between the vortex ratio and wave period. No published studies have found correlation between period and vortex ratios.

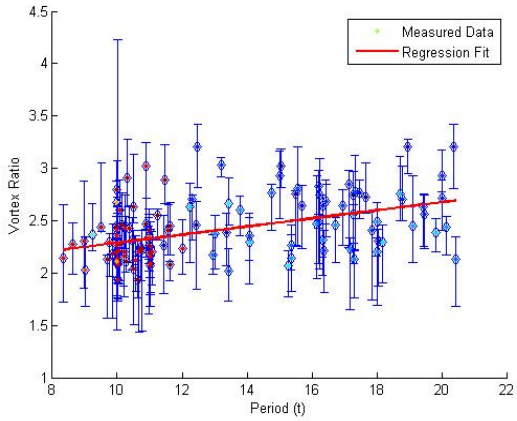

Fig. 9 Vortex Ratio Period Relationship

The Surf Similarity Parameter (SSP) differentiates between different breaking wave types and increasing SPP values are

theorised to give lower vortex ratios. As shown in Fig. 10a, a corroborating trend may be apparent within the data scatter yet the fitted trend line features an R^2 of only 0.14. However, a binned box plot of Fig. 10a shows no definite trend with respect to the SSP (Fig. 10b) and parameter independence.

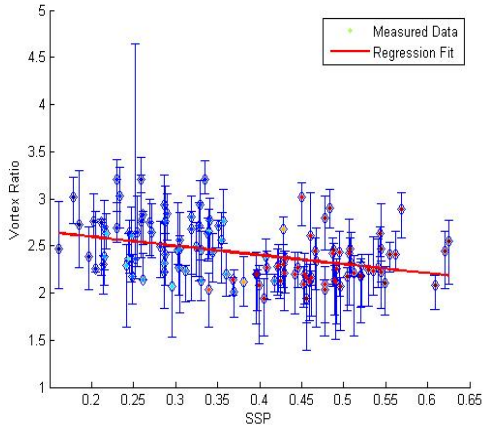

Fig. 10a Vortex Ratio VS SSP Relationship

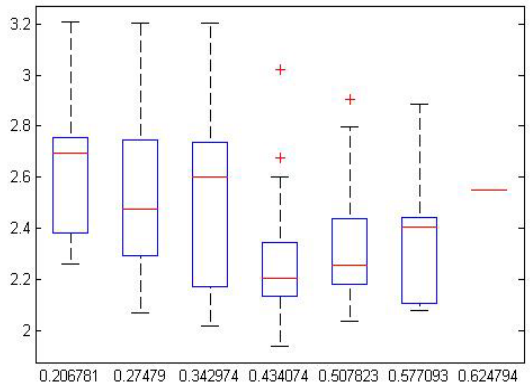

Fig. 10b Binned Vortex Ratio VS SSP plot

As summarized in Table III, the vortex ratio was rigorous analysed against all breaking wave and local bathymetric characteristics. No trend line found a correlation of determination above 0.28. As a result, no defining and significant relationships could be drawn from the collected data, corroborating the findings of Johnson [16], Blenkinsopp [29] and Grilli et al. [6]. These findings bring the suggestion that breaker vortex ratios may be good descriptor of breaking intensity into doubt.

In order to assess the application of the vortex angle as a breaking intensity predictor, a similar set of comparative plots were analysed. As shown in Table V, none of the relationships featured an R^2 value above 0.02 and all featured large RMSE.

TABLE V
VORTEX ANGLE DEPENDENCE OVERVIEW

Wave Vortex Angle Relationships				
	Constant	Slope	R-Square	Linear RMSE
ND Depth	46.76	-416.36	0.00	4.99
ND Wave Height	46.02	183.21	0.00	4.99
Seafloor Slope	44.46	54.05	0.02	4.93
Breaker Index	46.02	0.22	0.00	4.99
Period	48.27	-0.15	0.01	4.96
ND Height*Slope	45.70	12357.5	0.00	4.98
ND Depth*Slope	46.31	-1200	0.00	4.99
Breaker Steepness	43.27	83.85	0.01	4.96
SSP	44.14	5.58	0.02	4.94

The highest co-efficient of correlation values were found for seafloor slope and SSP plots, yet a basic visual analysis Fig. 11 and Fig. 12 show the high degree of data scatter and a lack of dependence. These findings corroborate previous laboratory investigations into breaker vortex angles have also indicate no significant trends [2, 5, 16]. It is suggested that the lack of angle dependence is due to increasing vortex angles, θ, during the progression of the breaking event, as theoretically predicted by Vinje and Brevig [30] and Longuet-Higgins [7].

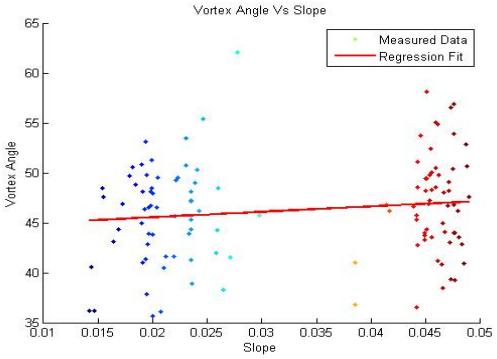

Fig. 11 Vortex Angle vs. Slope Relationship

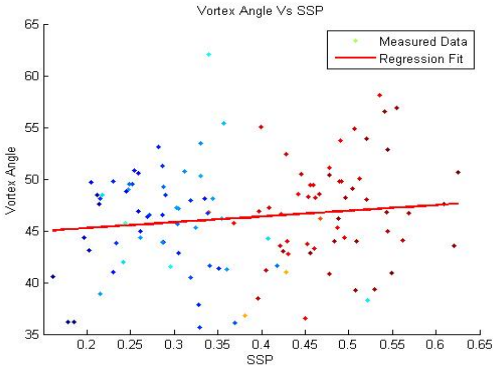

Fig. 12 Vortex Angle vs. SSP Relationship

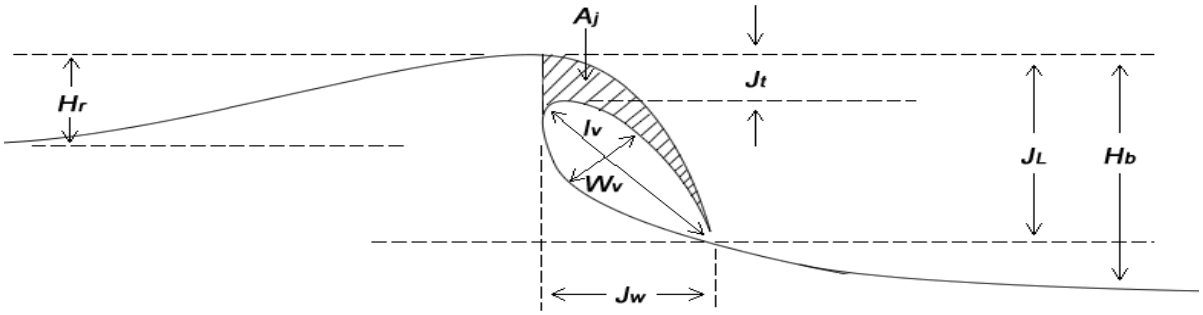

Fig. 13 Breaking Wave Geometric Parameters

V. Recommendations

Given that only consistent trend between published papers and the data presented in this study is a lack of dependence between vortex parameters and breaking wave conditions, it is concluded that the vortex angle and vortex ratios are not adequate to predict the breaking wave intensity.

Suggested below are a number of different geometric parameters which may provide better prediction of wave breaking intensity. It is predicted that the geometric prediction of intensity will be multi-parameter dependant, rather than solely predicted by any single parameter. See Fig. 12 for visual explanation of suggested parameters.

- *Jet Length / Breaker Height Ratio (J_L/H_b):* The authors analysis of Grilli et al's [6] profile images shows the jet length/break height ratio changing dramatically with seafloor slope. Ratios of 0.50, 0.80 and 1 for 1/100, 1/35 and 1/15 slopes respectively were measured, illustrating that the jet length ratios may be a relevant parameter in breaking intensity.

- *Rear Wave Height / Breaker Height Ratio (H_r/H_b):* Often qualitatively noted by surfer and ocean enthusiasts, the rear wave height/breaker height may provide additional insight into the breaking intensity.

- *Jet Thickness / Breaker Height Ratio (J_t/H_b) or Jet Area / Breaker Height ^{2} (A_j/H_b^2):* Grilli et al[6] suggested the area of the jet at touchdown may be a good measure of intensity. These parameters will provide a non-dimensionalised indication of the amount of water with the overturning jet and breaking intensity.

- *Jet Width / Breaker Height Ratio (J_w/H_b):* Wave speed in shallow water is directly correlated to depth, and since the jet width is directly correlated to the speed differential between the wave crest and the main bulk of the wave, this may provide additional information about the breaking intensity.

VI. Conclusion

In this paper, the feasibility of predicting breaking wave parameters for use as a descriptor of breaking wave intensity is investigated. A detailed field study was conducted to extract all breaking wave characteristics, including vortex parameters, allowing for the first full analysis of vortex parameters as breaking intensity predictors. Through a thorough investigation of all published studies involving vortex parameters and the data collected in this study, it is concluded that the use of the vortex ratio and vortex angle is insufficient to predict the breaking intensity of waves and should not be investigated further. With the sole exception of Mead and Black [2], no published studies have found any significant correlation between these parameters and breaking conditions, providing evidence to inconclusive nature of pure vortex ratio or angle descriptions.

It is recommended that any further studies dealing with geometric characteristics include detailed measurements of the suggested novel geometric properties and investigate a multi-parameter approach. However, the potential of reliably extracting the recommended parameters from field conditions is low. Given the necessity of a perfect profile image to extract the recommended parameters and the complex nature of breaking conditions, it is doubtful that detailed trends will be evident within the inherent uncertainty and scatter of this data collection method. Hence, the recommended parameters stand only as possible geometric descriptors of breaking intensity and it is suggested that purely geometric descriptors are both too variable and unstable for rigorous breaking wave intensity studies to be preformed.

References

[1] Iribarren, C.R. and C. Nogales, *Protection des Ports.* 17th International Navigation Congress, 1949. **2**: p. 31 - 80.

[2] Mead, S.T., Black, K., *Predicting the Breaking Intensity of Surfing Waves.* Special Issue of the Journal of Coastal Research on Surfing., 2001: p. 103 -130.

[3] Scarfe, B.E., et al., *The Science of Surfing Waves and Surfing Breaks - A Review.* Scripps Institution of Oceanography Technicial Report, 2003: p. 1 - 12.

[4] Smith, E.R. and N.C. Kraus, *Laboratory Study of Wave Breaking over Bars and Artificial Reefs.* Journal of Waterway, Port, Coastal and Ocean Engineering, 1991. **117**(4): p. 307 - 325.

[5] Blenkinsopp, C.E. and J.R. Chaplin, *The Effect of Relative Crest Submergence on Wave Breaking over Submerged Slopes.* Coastal Engineering, 2008. **55**: p. 967-974.

[6] Grilli, S.T., I.A. Svendsen, and R. Subramanya, *Breaking Criterion and Characteristics for Solitary Waves on Slopes.* Journal of Waterway, Port, Coastal and Ocean Engineering, 1997. **123**(3): p. 102 -112.

[7] Longuet - Higgins, M.S., *Parametric Solutions for Breaking Waves.* Journal of Fluid Mechanics, 1982. **121**: p. 403 - 424.

[8] Miller, R.L., *Role of Vortices in Surf Zone Prediction, Sedimentation and Wave Forces.* Beach and Nearshore Sedimentation (ed. R.A. Davis & R.L. Ethington), 1957: p. 92 - 114.

[9] New, A.L., *A Class of Elliptical Free-Surface Flows.* Journal of Fluid Mechanics, 1983. **130**: p. 219 - 239.
[10] Millar, R.L., *The Role of Surface Tension in Breaking Waves.* Coastal Engineering, 1972. **13**: p. 433 - 449.
[11] Shand, T.D., Bailey, D.G., Shand, R.D., *Automated Detection of Breaking Wave Height Using an Optical Technique.* Journal of Coastal Research, 2012.
[12] Gal, Y., Browne, M., Lane, C., *Automatic Estimation of Nearshore Wave Height from Video Timestacks.* 2011 International Conference on Digital Image Computing, 2011: p. 364 - 369.
[13] Almar, R., Cienfuegos, R., Catalan, P., Michallet, H., Castelle, B., Bonneton, P., Marieu, V. , *A New Breaking Wave Height Direct Estimator from Video Imagery.* Coastal Engineering, 2012. **61**: p. 42-48.
[14] Walker, J.R., *Recreational Surf Parameters.* LOOK Laboratory TR-30, University of Hawaii, Department of Ocean Engineering, Honolulu, Hawaii., 1974.
[15] Fairley, I. and M.A. Davidson, *A Two-Dimensional Wave Flume Investigation into the Effect of Multiple Steps on the Form of Breaking Waves.* Journal of Coastal Research, 2008. **24**(1): p. 51 - 58.
[16] Johnson, C.M., *The Effect of Artificial Reef Configerations on Wave Breaking Intensity Relating to Recreational Surfing Conditions.* MSc Thesis, Civil Engineering, University of Stellenbosch, 2009: p. 1 - 137.
[17] de Vries, S., de Schipper, M.A., Hill, D.F., Stive, M.J.F., *Remote Sensing of Surf Zone Waves Using Stereo Imaging.* Coastal Engineering, 2010: p. 1 - 12.
[18] Ritchie, A.C., Finlayson, D.P., Logan, J.B. *Swath bathymetry surveys of the Monterey Bay area from Point Año Nuevo to Moss Landing, San Mateo, Santa Cruz, and Monterey Counties, California*. U.S. Geological Survey 2010; Data Series 514]. Available from: http://pubs.usgs.gov/ds/514/.
[19] Flick, R.E., Guza, R.T., Inman, D.L., *Elevation and Velocity Measurements of Laboratory Shoaling Waves.* Journal of Geophysical Research, 1981. **86**: p. 4149 - 4160.
[20] Le Mehaute, B., Divoky, D., Lin, A., *Shallow Water Waves: A Comparision of Theories and Experiments.* Proceedings 11th Conference of Coastal Engineering, 1968. **1**.
[21] Lin, P., Philip, L,. Liu, F., *A numerical study of breaking waves in the surf zone.* Journal of Fluid Mechanics, 1998. **259**(239 - 264).
[22] Couriel, S., P. Horton, and D. Cox, *Supplementary 2D Physical Modelling of Breaking Wave Characteristics.* Technicial Report, Water Research Laboratory, 1998. **TR98-14**.
[23] CERC-EW, *Coastal Engineering Manual.* 2008. **EM-1110-2-1100**.
[24] Goda, Y., *Reanalysis of Regular and Random Breaking Wave Statistics.* Coastal Engineering Journal, 2010. **52**(1): p. 71 - 106.
[25] Rattanapitikon, W., T. Vivattanasirak, and T. Shibayama, *A Proposal of New Breaker Height Formula.* Coastal Engineering Journal, 2003. **45**(1): p. 29 - 48.
[26] Weggel, R., *Maximum Breaker Height for Design.* Proceedings of the International Conference on Coastal Engineering, 1972: p. 419 - 432.
[27] Rasband, W.S., *ImageJ*. 1997 - 2012, U.S. National Institutes of Health: Bethesda, Maryland, USA.
[28] Dumouchel, W., O'Brien, F., *Intergrating a robust option into a multiple regression computing environment.* Institute for Mathematics and Its Applications, 1991. **36**: p. 41.
[29] Blenkinsopp, C.E., *The Effect of Micro-Scale Bathymetric Steps on Wave Breaking and Implications for Artificial Surfing Reef Construction.* Proceedings of the 3rd International Surfing Reef Symposium, Raglan, New Zealand, 2003: p. 139 - 155.
[30] Vinje, T. and P. Brevig, *Numerical Simulation of Breaking Waves* Finite Elements in Water Resources, 1980. **2**: p. 196 - 210.